Domain wall dynamics during the devitrification of $Fe_{73.5}CuNb_3Si_{11.5}B_{11}$ magnetic microwires

J. Olivera,[1,2] R. Varga,[1,*] V. M. Prida,[2] M. L. Sanchez,[2] B. Hernando,[2] and A. Zhukov[3]
[1]*Institute of Physics, Faculty of Science, UPJS, Park Angelinum 9, 041 54 Kosice, Slovakia*
[2]*Department of Physics, University of Oviedo, Calvo Sotelo s/n, 33007 Oviedo, Spain*
[3]*Deptartamento de Fisica Materiales, Facultad de Quimica, UPV/EHU, 1072, 20080 San Sebastian, Spain*
(Received 22 March 2010; revised manuscript received 17 June 2010; published 9 September 2010)

We have studied the evolution of domain wall dynamics during the devitrification of amorphous and nanocrystalline $Fe_{73.5}Cu_1Nb_3Si_{11.5}B_{11}$ microwires. Depending on the annealing temperature range, three different regimes in the domain wall dynamics can be considered for these materials. Annealing below the Curie temperature, T_c, of the alloy leads to the stabilization of the domain structure and a strong temperature dependence of the domain wall dynamic parameters. However, annealing above T_c leads to a destabilization of domain patterns and a decrease in the domain wall damping in one order of magnitude. Finally, annealing above the crystallization temperature, T_x, leads to the appearance of the nanocrystalline state that is structurally very stable. In this case, the domain wall velocity is very fast due to the lack of magnetic anisotropy and extremely stable with the temperature.

DOI: 10.1103/PhysRevB.82.094414 PACS number(s): 75.60.Ej, 75.60.Jk

Domain wall dynamics in thin magnetic wires is currently used in modern spintronic devices to store (race-track memory, field driven domain wall motion memory) or transfer (domain wall logic, domain wall diode) information.[1–4] Generally, the domain wall propagation is forced either by an electrical current or by an applied magnetic field. However, the transfer or storage speed of such devices is determined by the domain wall velocity, which is given mainly by domain wall damping.

The amorphous glass-coated microwires are ideal materials to study the domain wall dynamics in a thin magnetic wire.[5] They are composite materials that consist of metallic nucleus (1–30 μm in diameter) covered by a glass coating (thickness of 2–20 μm).[6] Due to the lack of magnetocrystalline anisotropy, magnetoelastic and magnetostatic anisotropies are the most important determining the magnetic properties of amorphous microwires. During their fabrication, strong elastic stresses are induced in the microwire having axial direction in the center and radial direction just below the surface of the metallic nucleus.[7] As a result, the domain structure of amorphous microwires with positive magnetostriction consists of one single axial domain placed in the center of the wire (Fig. 1) that is surrounded by a radial domain structure just below the surface.[8] The peculiar domain pattern leads to a specific magnetization process that runs through the depining and subsequent propagation of a single domain wall (that is already present at the end of the wire even at $H=0$ in order to decreasing the stray fields).

The magnetization process consisting of the propagation of one single domain wall in a large scale of a few centimeter, together with the simple production control (composition, stresses, and anisotropy distribution) and dimensions of magnetic microwires make them outstanding materials for domain wall dynamics studies. Some of the most important previous results show that very fast domain wall motions can be observed due to the presence of low anisotropy.[9] In some cases, it has been observed that the domain wall velocity even gets over the sound speed in a metallic microwire.[10] When this occurs, the interaction of the domain wall with phonons leads to the "supersonic boom."[11] This avalanche effect can be employed to synchronize the multiple domain walls propagation in modern spintronic devices.

The advantages of the amorphous microwires, particularly the low magnetic anisotropy resulting from the lack of magnetocrystalline anisotropy, bring about a disadvantage related to their unstable amorphous structure that modifies the local anisotropy and leads to changes of all magnetic properties with time, temperature, etc. Amorphous materials are in a metastable state, so they can relax even at low temperatures.[5]

The solution of the above mentioned problem could be found by introducing a nanocrystalline structure in the metallic nucleus of microwire. Nanocrystalline alloys are composite materials that consist of crystalline grains of ~10 nm size randomly embedded in the amorphous matrix.[12] The total magnetocrystalline anisotropy is averaged out since the intrinsic exchange length (~35 nm) is longer than the diameter of the crystalline grain. Moreover, the negative magnetostriction of α-FeSi nanocrystallites is balanced by the positive magnetostriction of the remaining amorphous matrix. Thus, they exhibit an excellent magnetic softness due to the almost zero magnetostriction and vanishing crystalline anisotropy.[13]

Typical composition for nanocrystalline materials is based on the FeSiBNbCu (FINEMET alloy). Since its discovery in 1988,[14] there were a lot of attempts to employ this alloy in specimens with different geometry.[15] The development of nanocrystalline structure into the metallic nucleus of glass-covered microwires naturally favors both, the low anisotropy

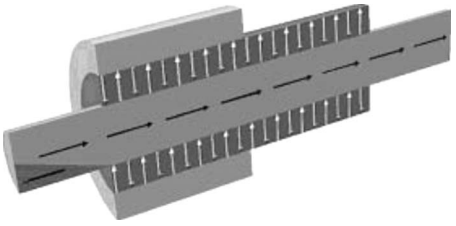

FIG. 1. Schematic domain structure of glass-coated microwire with positive magnetostriction.

needed for fast domain wall, and the high structural stability characteristic of the nanocrystalline state. In the present work we deal with the domain wall dynamics during the devitrification process of Finemet-based glass coated microwires.

Theory of the domain wall dynamics. Generally, the domain wall propagation in real magnetic materials can be described similarly to the linear harmonic oscillator under an external force $F(t)$ in a viscous medium.[16] Its time (t) dependent oscillation is described as

$$m\frac{d^2x}{dt^2}+\beta\frac{dx}{dt}+\xi x=F(t), \tag{1}$$

where m is the effective mass of the domain wall, β is the damping coefficient that characterizes the viscous medium, ξ is the stiffness coefficient, and x is the displacement of the domain wall from its equilibrium position. In the case of a domain wall, the force F is represented by a constant force, acting on the domain wall due to the applied magnetic field H and it is expressed as

$$F=b\mu_0 M_s H, \tag{2}$$

where b is a constant that depends on the domain wall configuration and is equal to 2 for 180° domain wall or $\sqrt{2}$ for 90° domain wall, μ_0 is the permeability of vacuum and M_s is the saturation magnetization.

Assuming the domain wall propagation at constant velocity ($d^2x/dt^2 \to 0$), a linear dependence of the domain wall velocity v on the applied magnetic field H can be simply obtained

$$v=S(H-H_0). \tag{3}$$

Here S is the so-called domain wall mobility and H_0 is the critical field, below which the domain wall propagation cannot be observed. Comparing Eqs. (1) and (3), it can be shown that domain wall mobility is inversely proportional to the domain wall damping parameter

$$S=\frac{b\mu_0 M_s}{\beta}. \tag{4}$$

Therefore, the most important parameter that controls the domain wall velocity is the domain wall damping. At the beginning, the only source of domain wall damping was assumed to arise from eddy currents[17]

$$\beta_e=\frac{4\mu_0^2 M_s^2 r_0}{\rho}\left(\ln\frac{r_0}{r_b}+\frac{8}{\pi^2}\right), \tag{5}$$

where $\rho(T)$ is the resistivity and r_0 and r_b the radii of the wire and the inner core domain, respectively.

However, the strong wall damping for highly insulated materials, such as ferrites, cannot be fully explained by the eddy current damping and another contribution must be taken into account. Such damping, originated from the magnetic relaxation of magnetic moments β_r, is inversely proportional to the domain wall width δ_w (Ref. 18)

$$\beta_r \approx \frac{\alpha}{|\gamma|\delta_w}\approx\frac{\mu_0 M_s}{\pi}\sqrt{\frac{K}{A}}\approx\frac{\mu_0 M_s}{\pi}\sqrt{\frac{3\lambda_s\sigma}{2A}}, \tag{6}$$

where α is the so-called Gilbert-damping parameter, γ is the gyromagnetic ratio, K is the magnetic anisotropy energy density, being a magnetoelastic one for amorphous microwires, A the exchange stiffness constant, λ_s the magnetostriction, and σ is the mechanical stress.

Anyway, neither eddy currents, nor magnetic relaxation could explain the observed strong variation with the temperature of domain wall damping for some ferrites and amorphous materials. An additional damping coefficient, β_s, was introduced in[5] describing the structural relaxation influence of the mobile defects on atomic scale

$$\beta_s \propto \tau\langle(\varepsilon_{eff})^2\rangle(c_0/kT)G(T,t), \tag{7}$$

where τ is the relaxation time of the defects, ε_{eff} is the interaction energy of the domain wall with the defects, c_0 is the defects number, k is Boltzman constant, and $G(T,t)$ is the so-called relaxation function $G(t)=1-exp(-t/\tau)$.[19]

Amorphous microwires are in metastable state and they can relax even at low temperatures. Hence the structural relaxation can influence the domain wall damping significantly[5,20] through the movement of mobile defects the atoms appearing in the vicinity of the so-called free volumes (here the free volumes are the volume fractions with the volume density lower than the average one[21]) that decrease their interaction energy with local magnetization.

In contrary to previous contributions (eddy current and magnetic relaxation) to the domain wall damping, the structural relaxation component can be modified by properly setting the experimental conditions or by thermal treatment.[22] During the experiment, three time parameters are important. (1) τ_r—relaxation time due to defects (given by Arrhenius law: $\tau_r=\tau_0\, exp(Q/kT)$, where τ_0 is the pre-exponential factor, Q is the activation energy of the defect and k is the Boltzmann constant[19]). (2) t_1—time necessary to propagate the domain wall across the defect (given by the domain wall width and its velocity). (3) t_2—time between two domain wall propagations [given by the frequency f of the applied magnetic field H, $t_2 \sim 1/f$; $t_2=t$ in Eq. (7)].

The relative value of τ_r with respect to t_1 and t_2 determines five thermal ranges for the domain wall propagation.[23] (1) Metastable range: $\tau_r > t_2 > t_1$. Defects have no time to relax (they are frozenlike) and they appear in the nonthermodynamical equilibrium. The amplitude of the structural relaxation damping is given by the history of the material. If the material is stabilized, by annealing below the Curie temperature, β_s is high but if the system is destabilized, by demagnetization or by heating above the Curie temperature, β_s is small. Such range corresponds to low temperatures (see Arrhenius law). (2) Structural relaxation range: $\tau_r \sim t_2 > t_1$. Defects are able to relax between two domain wall propagations. This makes β_s increase hindering the domain wall propagation. By properly setting the driving frequency, that range can be moderated and the structural relaxation damping β_s can be increased or decreased.[24] (3) Adiabatic range: $t_2 > \tau_r > t_1$. The defects system is in thermal equilibrium and β_s reaches a maximum, at a given temperature [see Eq. (7)]

but the defect cannot follow the propagating domain wall. (4) Diffusion-damped range: $t_2 > t_1 \sim \tau_r$. In this regime, the time that it takes for the domain wall to cross a single defect is comparable to its relaxation time. The defect relaxes during the domain wall propagation thus decreasing the domain wall speed. By increasing the applied field amplitude, the domain wall velocity rises until $t_1 < \tau_r$, when the domain wall is able to depin from the defect and goes into the adiabatic regime.[25] (5) Isothermal range: $t_2 > t_1 > \tau_r$. Although the whole system relaxes between two domain wall propagations, the relaxation time of defects is short and they are able to follow rapidly the domain wall during its propagation. β_s is small and the domain wall velocity increases. Such regime corresponds to high temperatures.

I. EXPERIMENT

The Finemet microwires with nominal composition $Fe_{73.5}Cu_1Nb_3Si_{11.5}B_{11}$ having a metallic nucleus of 10 μm diameter and a glass coating with a diameter of 28 μm, were cut into 9 cm long pieces. Samples were annealed in a furnace, for 1 h in an Argon atmosphere. The annealings were performed at temperatures of 473, 673, and 823 K. Domain wall motion measurements were made using the Sixtus-Tonks experiment.[5] The setup consists of three coaxial coils, a primary coil (10 cm long and 8 mm in diameter) and two pickup coils (3 mm long and 0.5 mm inner diameter each) symmetrically placed inside that are separated by a distance of 6 cm between them and connected in series opposition. The magnetizing coil was driven by a 10 Hz frequency square wave that creates a homogeneous field along the wire. Two sharp peaks are picked up with an oscilloscope when the propagating wall passing across the two sensing coils. The domain wall velocity can be calculated from $v = L/\Delta t$, where L is the distance between pickup coils and Δt is the time interval between the two peaks happen. The system is placed inside a specially designed cryostat system enabling the measurement in the temperature range from 77 to 380 K. More experimental details can be found elsewhere.[10]

Magnetization measurements as a function of temperature were performed by a superconducting quantum interference device magnetometer with 1 cm long samples in 1T applied magnetic field, high enough to saturate the magnetization of the samples. Hysteresis loops were measured at different temperatures in the same magnetometer for applied fields up to 2 T.

II. RESULTS

The domain wall dynamics of as-cast amorphous FeSiBNbCu microwires has been studied previously.[26] The domain wall mobility was quite high and very fast domain wall velocities have been achieved (2000 m/s). Two regions in the domain wall dynamics have been observed with different domain wall structure: transversal and vortex one. However, the domain wall damping varies strongly with the temperature. The amorphous alloys are in a metastable state. Hence they can relax even at low temperatures, which also modify the parameters of the domain wall dynamics. Here, we study the effect of the thermal treatment on the domain wall dynamics in order to stabilize it. Before starting, we must explain some peculiarities arising from the thermal treatment of glass-coated microwires. First, the glass coating introduces additional stresses on the metallic nucleus. Such stresses, $\sigma_a(T)$, are caused by the different thermal expansion coefficient of metallic nucleus, α_m, and glass coating, α_g, and are proportional to the temperature change ΔT (Ref. 27)

$$\sigma_a(T) \approx E(\alpha_g - \alpha_m)\Delta T, \tag{8}$$

where E is the Young modulus. As a consequence, although the stresses could relax at higher temperature during the heat treatment, when cooling the sample down to room temperature new stresses are introduced.

Another peculiarity comes up from the annealing temperature. Annealing the sample below its Curie temperature, around 330 °C for Finemet microwire,[28] the magnetic annealing could lead to the induction of a local magnetic anisotropy.[19,29] Annealing above the Curie temperature leads to the rearrangement of the locally induced magnetic anisotropy. While annealing above the Crystallization temperature, T_x, a complete change in the microwire structure is achieved. Therefore we divide our results into three main groups.

A. Annealing at 473 K for 1 h (below T_C)

The annealing below the Curie temperature of the alloy usually leads to a strong induced anisotropy in amorphous microwires. During such annealing, the existing domain pattern is stabilized. As a consequence, due to the decrease in the domain wall mobility the initial susceptibility diminishes[30] and a higher critical field must be applied to remove the domain wall from their equilibrium position.[31] The largest effect of such stabilization is typically observed at around 473 K.[26]

The domain wall dynamics of one FeSiBNbCu microwire heat treated at 473 K is shown in Fig. 2(a). As in almost all cases in microwires,[5,32] the domain wall velocity v is found to be exactly proportional to the applied field H according to Eq. (3). Thus, these microwires are ideal materials for domain wall dynamics studies. However, some peculiarities are found in that dynamics. First, the domain wall velocity decreases with measuring temperature, which is quite controversial in comparison with previous results.[5,33] Typically, the magnetic moments freedom increases with the temperature due to their thermal activation and so does the domain wall velocity. Furthermore, the domain wall velocity is mainly driven by two parameters: the domain wall mobility S, which is inversely proportional to the domain wall damping β and the critical propagation field, H_0. Although the domain wall mobility S decreases at low temperature, the domain wall velocity remains high due to the large and negative critical propagation field.

The negative value of the critical propagation field H_0 still remains as a controversial parameter in the domain wall dynamics. Theoretically, the critical propagation field should be proportional to the pinning strength,[1,16] therefore it should be always positive. However, negative critical propagation field

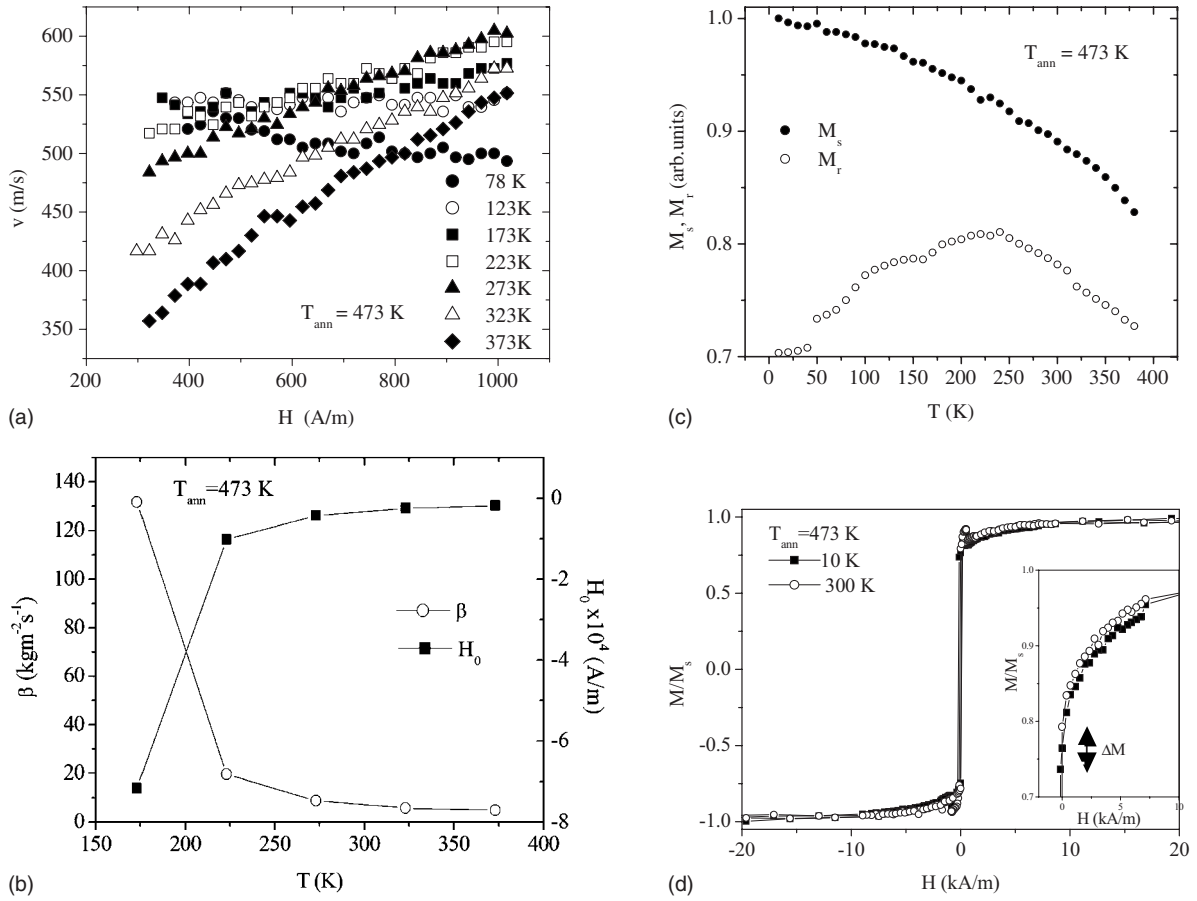

FIG. 2. (a) Domain wall dynamics of FeSiBNbCu microwire annealed at 473 K for 1h, with the measuring temperature as a parameter. (b) Temperature dependence of domain wall damping and critical propagation field for the FeSiBNbCu microwire annealed at 473 K for 1h. (c) Temperature dependence of saturation (M_s) and remanent (M_r) magnetization for the FeSiBNbCu microwire annealed at 473 K for 1h. (d) Hysteresis loops measured at 10 and 300 K for the FeSiBNbCu microwire annealed at 473 K for 1h.

values have been previously measured in magnetic microwires[5,9,32] and also in ferrites,[34] and the reason for such a phenomenon was postulated to be a dramatic change in the domain wall structure before it can begin to move.[34] In fact, the domain wall dynamics does not remain in the viscous regime below the lowest applied field and changes its field dependence from a linear to a power law.[20]

As opposite to the domain wall velocity, the wall mobility S increases with the temperature. According to the Eq. (4), the wall mobility is mainly driven by the domain wall damping because the saturation magnetization decreasing with temperature in the measured temperature range, [see Fig. 2(c)]. As shown in Fig. 2(b), the domain wall damping strongly increases at low temperature and reaches even negative values at around 78 K. Taking into account that the domain wall dynamics is similar to the dislocation dynamics in real crystals[35] and in shape memory alloys,[36] or the dynamics of tectonic plates,[37] etc., the negative value of the domain wall damping is always an interesting effect. It indicates that the higher the force acting on the domain wall is, the slower the domain wall propagation is.

Negative domain wall mobility has been already predicted by Walker[38] and measured in different magnetic wires.[39] It can appear at large applied fields, above the so-called Walker limit, when the domain wall propagation is not in the viscous regime anymore. Instead of that, something like a turbulent propagation of the domain wall appears. The field value, at which the Walker limit takes place, is called Walker field and depends on the anisotropy (axial or transversal) present in the sample. However, the negative domain wall mobility here present could be ascribed to the diffusion-damped domain wall propagation. As was shown in,[24,25] it results from the structural relaxation contribution to the domain wall damping after annealing below T_C, and can be overcome by increasing the driving frequency, decreasing the time for the defects relaxation.

As mentioned above, the annealing below T_C has two effects. First, the domain structure is stabilized through the locally induced magnetic anisotropy. However, when the sample is cooled down to the room temperature, other stresses are applied by the glass coating as given by Eq. (8). Such stresses, axial and/or radial, affect the stabilized domain pattern. Some idea about the domain structure can be obtained from the temperature dependence of saturation M_s and remanent M_r magnetization along the microwire axis [Fig. 2(c)]. Assuming the domain structure of microwire as given in Fig. 1, the saturation magnetization M_s is proportional to the contribution of magnetic moments in the whole volume of the metallic nucleus of the microwire whereas the remanent magnetization M_r is proportional to contribution of

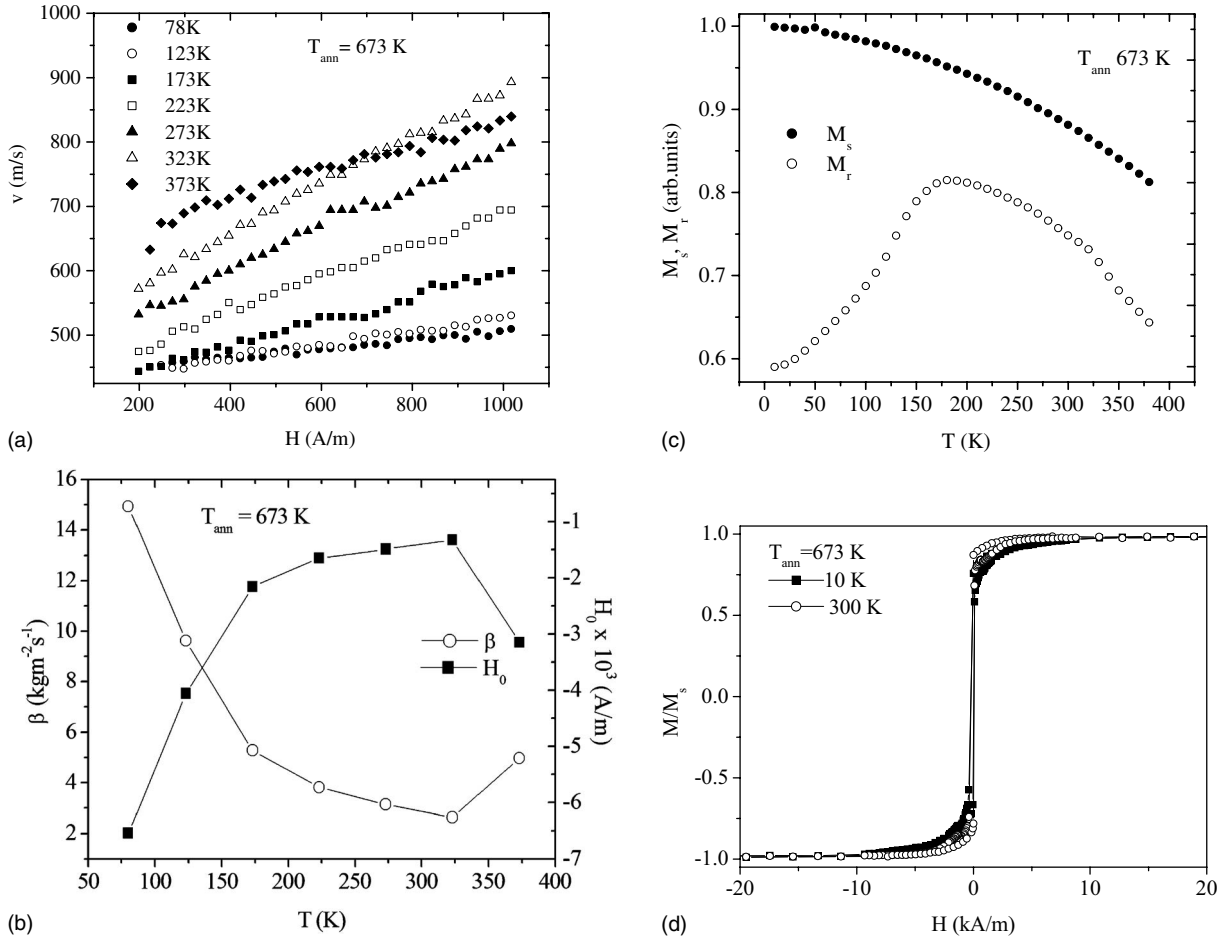

FIG. 3. (a) Domain wall dynamics of FeSiBNbCu microwire annealed at 673 K for 1h, with the measuring temperature as a parameter. (b) Temperature dependence of domain wall damping and critical propagation field for the FeSiBNbCu microwire annealed at 673 K for 1h. (c) Temperature dependence of saturation (M_s) and remanent (M_r) magnetization for the FeSiBNbCu microwire annealed at 673 K for 1h. (d) Hysteresis loops measured at 10 and 300 K for the FeSiBNbCu microwire annealed at 673 K for 1h.

magnetic moments located in the volume of single axially magnetized domain in the core of the wire. The difference between them corresponds to the contribution of magnetic moments located in the shell (radial domain structure). It can be seen that the volume of the axially magnetized domain remains constant in the temperature range from 250 to 400 K. However, as the temperature is decreased below 250 K the radial stress distribution is favored, which is confirmed by an increase in thickness of the radial domain structure. This is also confirmed by measuring the hysteresis loops [Fig. 2(d)]. Applied fields higher than 10 kA/m become necessary in order to saturate the microwire. The relative volume of the radial structure increases over 25% of the whole metallic nucleus at 10 K, in comparison with 300 K when it only occupies 20% [see inset in Fig. 2(d)]. Moreover, higher fields are necessary to saturate the microwire at 10 K because of the higher radial anisotropy.

Anyway, it is clear from comparison between Figs. 2(b) and 2(c) that the increase in domain wall damping at low temperature is related to induced stresses, which also modify the domain structure.

B. Annealing at 673 K for 1 h (above T_C and below T_x)

Annealing above T_C has a few effects on the structure of FeSiBNbCu microwires. Such a temperature is high enough to release the stresses induced during the fabrication procedure, leading to an anisotropy homogenization of the material and consequently, the coercivity decreases.[28] The domain structure disappears above the Curie temperature, hence the local defects will be randomly distributed making the domain structure destabilized. It is manifested by very small pinning field.[31] However, the FeSiBNbCu microwire still remains in amorphous state, therefore its structural relaxation occurs even at low temperatures.[29]

Thus, the domain wall dynamics is similar to the corresponding one in the as-cast microwire. The domain wall velocity increases with the temperature and so does the domain wall mobility [Fig. 3(a)].

Second, the annealing at such high temperature leads to the stress relief and homogenization of the structure. In fact, annealing at 673 K leads to a maximum decrease in the switching field in amorphous Finemet microwire[40] and the domain wall velocity increases comparing to that of the microwire annealed at 473 K.

However, additional stresses are induced on the metallic nucleus by glass coating due to their different thermal expansion coefficient when the microwire is cooled down to room temperature [see Eq. (8)].

In this case, the domain wall damping is around one order of magnitude lower than that after annealing at 473 K and decreases with temperature [Fig. 3(b)]. It could be ascribed to the lower local anisotropy due to the random redistribution of the defects after annealing at temperature above T_C. Moreover, the decrease in the domain wall damping due to the diminishing of the mobile defects concentration c_0 given by Eq. (7) should be also taken into account as has been already found for FeSiB microwires annealed at 673 K.[22]

While the critical propagation field remains negative [Fig. 3(b)], its amplitude is about one order of magnitude lower than the value for the microwire annealed at 473 K, probably due to the higher stress relaxation.

The most important parameters controlling the domain wall dynamics, according to Eqs. (6) and (8), are the distribution and strength of induced stresses on the metallic nucleus by the glass coating. One can see from Fig. 3(c) that the domain structure remains constant in the temperature range between 175 and 375 K. Below this range, the radial domain structure in the shell increases in volume [Fig. 3(c)]. The annealing temperature at 673 K is high enough (in comparison with the one at 473 K) to relax significantly the stresses induced during the microwire fabrication. Hence, the effect of the stresses induced by glass coating when the temperature cools down to RT is stronger. This is also confirmed by measuring the hysteresis loops at the relevant temperatures [Fig. 3(d)]. The microwire reaches the saturation magnetization state for an applied field value of 5 kA/m at 300 K but higher magnetic field values above 10 kA/m must be applied at 10 K to saturate the sample. However, although the variation in the axial core domain volume is higher than for the microwire annealed at 473 K, the temperature dependence of the domain wall damping together with the variation in the critical propagation field are not as so high that in the case of the microwire annealed below T_C. This points out the fact that the locally induced magnetic anisotropy through the structural relaxation [Eq. (7)] is the dominant factor in determining the domain wall velocity at least in amorphous materials, which allows the existence of structural relaxation even at low temperatures.[19,31] The annealing at 673 K significantly reduces the mobile defect concentration c_0 [given in Eq. (7)] with respect to annealing process at lower temperature.[31] Therefore, the effect of structural relaxation on the domain wall dynamics is weaker than in the case of annealing at 473 K.

C. Annealing at 823 K for 1 h (above T_x)

The fastest domain wall value of 1000 m/s has been found for the microwire annealed at 823 K. The annealing treatment at 823 K leads to the development of the nanocrystalline microstructure that consists of α-FeSi grains randomly distributed into an amorphous matrix.[6] The nanocrystalline structure in the material has some advantages. First, the random orientation of the nanocrystalline grains are interexchange-coupled averaging out the magnetocrystalline anisotropy since their diameter is much smaller than the exchange correlation length.[12] Moreover, the crystalline α-FeSi grains have a negative magnetostriction coefficient in contrary to the positive one of the amorphous matrix. Thus, the effective magnetostriction of nanocrystalline FeSiBNbCu microwire is nearly zero and a negligible role in the magnetic properties is played on the nanocrystallized material by the magnetoelastic anisotropy. Therefore, a large magnetic susceptibility and very low-switching field are characteristic properties of nanocrystalline material.[41]

As a consequence of the low anisotropy, the domain wall velocity reaches a high value above 1000 m/s for rather low applied magnetic field of 1000 A/m [Fig. 4(a)]. The highest domain wall velocity measured in thin crystalline ferromagnetic wires was about 1500 m/s in a FeNi microwire, although it was reached for a much larger applied magnetic field of around 4000 A/m.[42] Moreover, the low anisotropy results in a small domain wall damping value less than 2.5 kg m^{-2} s^{-1} that does not change significantly with the temperature because of the stable crystalline structure developed in the material [Fig. 4(b)]. Vanishing magnetocrystalline and magnetoelastic anisotropies are confirmed also by magnetization measurements [Fig. 4(c)]. The single-domain structure (given in Fig. 1) is confirmed only in the temperature range from 250 to 325 K. Outside this range, the single-domain structure is destroyed, which is confirmed not only by the sharp decrease in the remanent magnetization [Fig. 4(c)] but hysteresis loops measurement [Fig. 4(d)]. Besides, the shape anisotropy strongly influences the domain structure of nanocrystalline FeSiBNbCu microwires. It must be pointed out that 1 cm long samples were used for magnetization measurement whereas 10 cm long samples were employed for domain wall damping measurements that clearly show magnetic bistability (i.e., single-domain structure). The critical length, to observe the magnetic bistability, given by domain wall structure shown in Fig. 1, is typically on the order of a few mm for highly magnetostrictive microwires.[43] For low-magnetostriction nanocrystalline FINEMET microwires, a length of sample of around 1 cm is not enough for the magnetic bistability occurs.

Due to the vanishing values of both magnetocrystalline and magnetoelastic anisotropies, the most important parameter governing the domain wall damping arises from the eddy current. Nanocrystalline microwires have much lower resistivity comparing to the amorphous ones.[44] Thus, the small decreasing of the domain wall damping with the temperature can be ascribed to the temperature dependence of the resistivity in nanocrystalline FeSiBNbCu microwires.

Although the domain wall damping slightly changes with temperature, the domain wall velocity increases due to the temperature dependence of the critical propagation field H_0, which also remains negative in the nanocrystalline state. However, its amplitude is one order of magnitude lower than that the value obtained after annealing at 673 K, and two orders of magnitude lower than that the corresponding one after annealing at 473 K.

III. CONCLUSIONS

To conclude, we have studied the effect of devitrification on the domain wall dynamics in amorphous and nanocrystal-

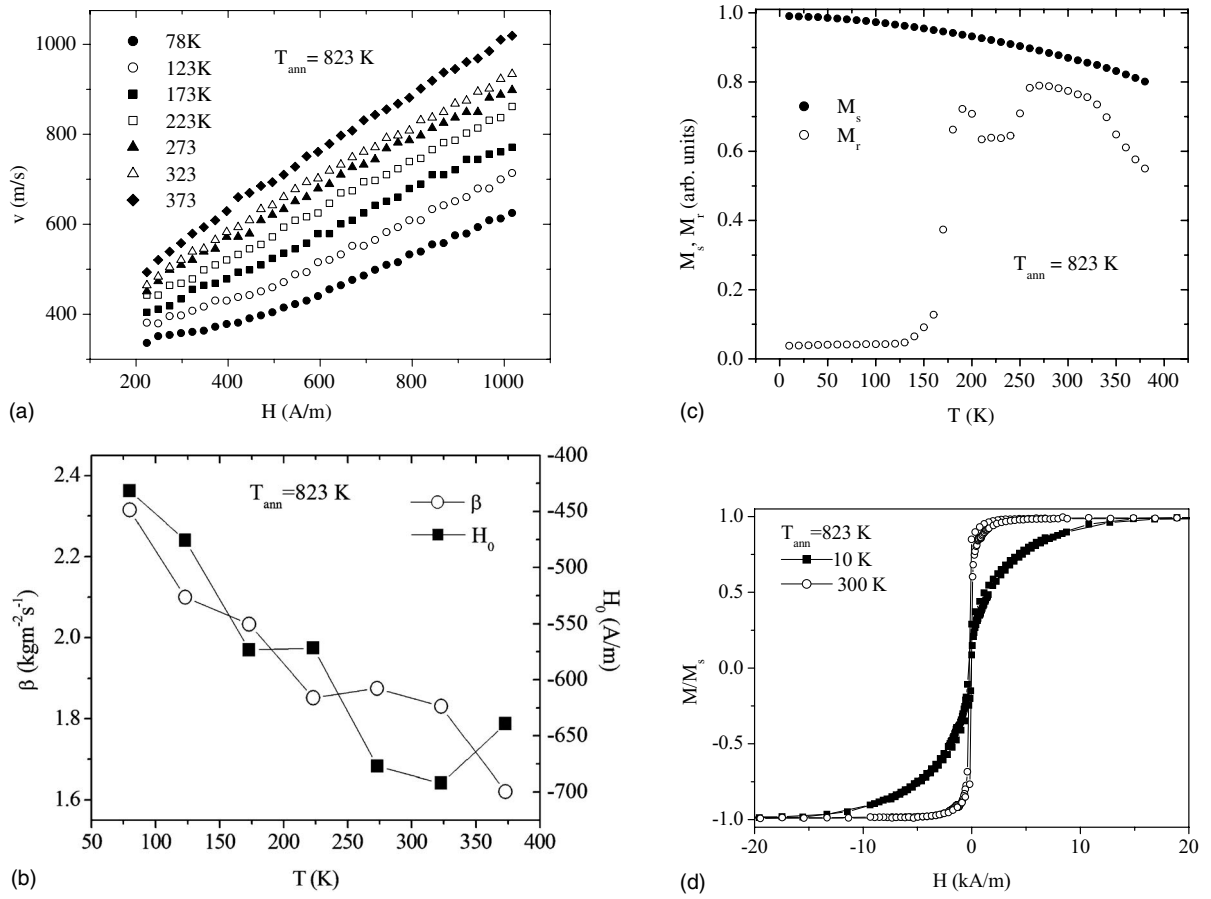

FIG. 4. (a) Domain wall dynamics of FeSiBNbCu microwire annealed at 823 K for 1h, with measuring temperature as a parameter. (b) Temperature dependence of domain wall damping and critical propagation field for the FeSiBNbCu microwire annealed at 823 K for 1h. (c) Temperature dependence of saturation (M_s) and remanent (M_r) magnetization for the FeSiBNbCu microwire annealed at 823 K for 1h. (d) Hysteresis loops measured at 10 and 300 K for FeSiBNbCu microwire annealed at 823 K for 1h.

line FeSiBNbCu glass-coated microwires. The domain wall dynamics in amorphous microwires is strongly dependent on temperature reflecting the change in magnetoelastic interaction and local rearrangement of their amorphous structure.

Annealing below the Curie temperature of the alloy leads to the stabilization of the domain structure resulting in a relatively slow domain wall motion. The domain wall damping decreases with temperature and was found to be negative for the lowest temperatures.

Annealing above the Curie temperature leads to the relaxation of the stresses and destabilization of the domain wall structure. As a consequence, the domain wall damping decreases by one order of magnitude. However, it remains temperature dependent due to its sensibility to the stress applied by a glass-coating when cooling down.

Annealing above the crystallization temperature leads to the formation of a stable nanocrystalline microstructure with vanishing magnetocrystalline as well as negligibly magnetoelastic anisotropy. Hence, the domain wall damping is mainly driven by the eddy current contribution that changes slightly with temperature. This results in a very stable domain wall dynamics with almost constant and low domain wall damping together with a quite fast domain wall displacement. Domain wall velocities of around 1000 m/s are among the highest observed in crystalline wires, however, they were obtained at much lower applied field values of 1000 A/m.

ACKNOWLEDGMENTS

This work was supported by the scientific grants Nano-CEXmat No. ITMS 26220120019, VEGA 1/0076/09, MICINN No. MAT2009-13108-C02-01 and FICyT No. FC09-IB09-131, Eu ERA-NET programme under DEVMAGMIWIRTEC (MANUNET-2007–Basque-3) and by the Basque Government under Saiotek 09 MicMagn project. J.O. acknowledges also the financial support from Spanish MEC.

*Corresponding author; rvarga@upjs.sk

[1] S. S. Parkin, M. Hayashi, and L. Thomas, Science **320**, 190 (2008).
[2] C. Y. You, Appl. Phys. Lett. **92**, 152507 (2008).
[3] D. A. Allwood, G. Xiong, C. C. Faulkner, D. Atkinson, D. Petit, and R. P. Cowburn, Science **309**, 1688 (2005).
[4] D. A. Allwood, G. Xiong, and R. P. Cowburn, Appl. Phys. Lett. **85**, 2848 (2004).
[5] R. Varga, K. L. Garcia, M. Vazquez, and P. Vojtanik, Phys. Rev. Lett. **94**, 017201 (2005).
[6] A. Zhukov, J. Gonzalez, M. Vazquez, V. Larin, and A. Torcunov, in *Encyclopedia of Nanoscience and Nanotechnology*, edited by H. S. Nalwa (American Scientific, Stevenson Ranch, CA, 2004), Chap. 62, p. 23.
[7] H. Chiriac, T. A. Ovari, and G. Pop, Phys. Rev. B **52**, 10104 (1995).
[8] J. Olivera, M. Provencio, V. M. Prida, B. Hernando, J. D. Santos, M. J. Perez, P. Gorria, M. L. Sanchez, and F. J. Belzunce, J. Magn. Magn. Mater. **294**, e163 (2005).
[9] R. Varga, A. Zhukov, J. M. Blanco, M. Ipatov, V. Zhukova, J. Gonzalez, and P. Vojtaník, Phys. Rev. B **74**, 212405 (2006).
[10] R. Varga, A. Zhukov, V. Zhukova, J. M. Blanco, and J. Gonzalez, Phys. Rev. B **76**, 132406 (2007).
[11] R. Varga, K. Richter, and A. Zhukov, IEEE Trans. Magn. **44**, 3925 (2008).
[12] G. Herzer, IEEE Trans. Magn. **26**, 1397 (1990).
[13] M. Tejedor, B. Hernando, M. L. Sanchez, V. M. Prida, J. M. Garcia-Beneytez, M. Vazquez, and G. Herzer, J. Magn. Magn. Mater. **185**, 61 (1998).
[14] Y. Yoshizawa, S. Oguma, and K. Yamauchi, J. Appl. Phys. **64**, 6044 (1988).
[15] C. Dudek, A. L. Adenot-Engelvin, F. Bertin, and O. Acher, J. Non-Cryst. Solids **353**, 925 (2007).
[16] C. W. Chen, *Magnetism and Metallurgy of Soft Magnetic Materials* (Dover, New York, 1986), p. 154.
[17] D. X. Chen, N. M. Dempsey, M. Vazquez, and A. Hernando, IEEE Trans. Magn. **31**, 781 (1995).
[18] H. J. Williams, W. Shockley, and C. Kittel, Phys. Rev. **80**, 1090 (1950).
[19] H. Kronmuller and M. Fahnle, *Micromagnetism and the Microstructure of the Ferromagnetic Solids* (Cambridge University Press, Cambridge, 2003), p. 274.
[20] R. Varga, J. Torrejon, Y. Kostyk, K. L. Garcia, G. Infantes, G. Badini, and M. Vazquez, J. Phys.: Condens. Matter **20**, 445215 (2008).
[21] H. Kronmüller, Phys. Status Solidi B **127**, 531 (1985).
[22] R. L. Novak, J. P. Sinnecker, and H. Chiriac, J. Phys. D **41**, 095005 (2008).
[23] L. M. Garcia, J. Bartolome, F. J. Lazaro, C. de Francisco and J. M. Munoz, Phys. Rev. B **54**, 15238 (1996).
[24] G. Infante, R. Varga, G. A. Badini-Confalonieri, and M. Vázquez, Appl. Phys. Lett. **95**, 012503 (2009).
[25] R. Varga, G. Infante, G. A. Badini-Confalonieri, and M. Vázquez, J. Phys.: Conf. Ser. **200**, 042026 (2010).
[26] J. Olivera, R. Varga, P. Vojtanik, V. M. Prida, M. L. Sanchez, B. Hernando, and A. Zhukov, J. Magn. Magn. Mater. **320**, 2534 (2008).
[27] R. Varga, K. L. Garcia, A. Zhukov, M. Vazquez, and P. Vojtanik, Appl. Phys. Lett. **83**, 2620 (2003).
[28] R. Varga, C. Luna, A. Zhukov, M. Vazquez, P. Vojtanik, Czech. J. Phys. **54**, D177 (2004).
[29] H. Kronmüller, Phys. Status Solidi B **118**, 661 (1983).
[30] P. Vojtaník, E. Komova, R. Varga, R. Matejko, R. Grossinger, H. Sassik, P. Agudo, M. Vazquez, and A. Hernando, J. Phys. IV **08**, Pr2-111 (1998).
[31] R. Grossinger, D. Holzer, C. Kussbach, H. Sassik, R. Sato Turtelli, J. P. Sinnecker, and E. Wittig, IEEE Trans. Magn. **31**, 3883 (1995).
[32] M. Neagu, H. Chiriac, E. Hristoforou, I. Darie, and F. Vinai, J. Magn. Magn. Mater. **226-230**, 1516 (2001).
[33] R. Varga, A. Zhukov, N. Usov, J. M. Blanco, J. Gonzalez, V. Zhukova, and P. Vojtanik, J. Magn. Magn. Mater. **316**, 337 (2007).
[34] T. H. O'Dell, *Ferromagnetodynamics* (The MacMillan Press, New York, 1981), p. 5.
[35] D. M. Dimiduk, C. Woodward, R. LeSar, and M. D. Uchic, Science **312**, 1188 (2006).
[36] R. Kainuma, Y. Imano, W. Ito, Y. Sutou, H. Morito, S. Okamoto, O. Kotakami, K. Oikawa, A. Fujita, T. Kanomata, and K. Ishida, Nature (London) **439**, 957 (2006).
[37] J. P. Sethna, K. A. Dahmen, and C. R. Myers, Nature (London) **410**, 242 (2001).
[38] N. L. Schryer and L. R. Walker, J. Appl. Phys. **45**, 5406 (1974).
[39] G. S. D. Beach, C. Nistor, C. Knutson, M. Tsoi, and J. L. Erskine, Nature Mater. **4**, 741 (2005).
[40] V. Zhukova, A. F. Cobeno, A. Zhukov, J. M. Blanco, V. Larin, and J. Gonzalez, Nanostruct. Mater. **11**, 1319 (1999).
[41] J. Arcas, C. Gomez Polo, A. Zhukov, M. Vazquez, V. Larin, and A. Hernando, Nanostruct. Mater. **7**, 823 (1996).
[42] D. Atkinson, D. A. Allwood, G. Xiong, M. D. Cooke, C. C. Faulkner, and R. P. Cowburn, Nature Mater. **2**, 85 (2003).
[43] M. Vázquez, Physica B **299**, 302 (2001).
[44] P. Klein, R. Varga, P. Vojtanik, J. Kovac, J. Ziman, G. A. Badini-Confalonieri, and M. Vazquez, J. Phys. D **43**, 045002 (2010).